TISSUE ENGINEERING: Part A
Volume 19, Numbers 19 and 20, 2013

DOI: 10.1089/ten.tea.2012.0393

Cells Behave Distinctly Within Sponges and Hydrogels Due to Differences of Internal Structure

Jingjing Zhang, BS,[1] Zheng Yang, PhD,[2] Chao Li, BS,[1] Yana Dou, BS,[3] Yijiang Li, BS,[1] Tanushree Thote, BS,[4] Dong-an Wang, PhD,[5] and Zigang Ge, PhD[1,3]

Different forms of biomaterials, including microspheres, sponges, hydrogels, and nanofibers, have been broadly used in cartilage regeneration; however, effects of internal structures of the biomaterials on cells and chondrogenesis remain largely unexplored. We hypothesized that different internal structures of sponges and hydrogels led to phenotypic disparity of the cells and may lead to disparate chondrogenesis. In the current study, the chondrocytes in sponges and hydrogels of chitosan were compared with regard to cell distribution, morphology, gene expression, and production of extracellular matrix. The chondrocytes clustered or attached to the materials with spindle morphologies in the sponges, while they distributed evenly with spherical morphologies in the hydrogels. The chondrocytes proliferated faster with elevated gene expression of collagen type I and down-regulated gene expression of aggracan in sponges, when compared with those in the hydrogels. However, there was no significant difference of the expression of collagen type II between these two scaffolds. Excretion of both glycosaminoglycan (GAG) and collagen type II increased with time *in vitro*, but there was no significant difference between the sponges and the hydrogels. There was no significant difference in secretion of GAG and collagen type II in the two scaffolds, while the levels of collagen type I and collagen type X were much higher in sponges compared with those in hydrogels during an *in vivo* study. Though the chondrocytes displayed different phenotypes in the sponges and hydrogels, they led to comparable chondrogenesis. An optimized design of the biomaterials could further improve chondrogenesis through enhancing functionalities of the chondrocytes.

Introduction

The incidence of cartilage injuries and cartilage degeneration increases as more people get involved in sports and as the aging population increases. With the lack of regenerative capacity of cartilage, intervention strategy in the form of surgical implantation or cell therapy needs to be employed to maintain and restore the mobility of patients.[1,2] Cartilage tissue engineering has achieved fairly good progress by using cells, scaffold/biomaterial, and growth factors in different forms.[3,4] Ideally, a biomaterial scaffold used for tissue engineering should have multiple roles, which include (1) providing structural support and guiding anisotropic-layered structures for *de novo* cartilage; (2) serving as a carrying vehicle for cells and/or growth factors; (3) guiding cell distribution and aggregation while providing microenvironments for cells; (4) transducing proper mechanical signals to individual cells; (5) facilitating nutrition exchange; and (6) guiding neo-tissue formation with simultaneous degradation, during regeneration and functionality of cartilage. In this regard, a variety of biomaterials have been designed and fabricated. Based on their internal structures, biomaterials can be classified into four categories: porous sponges,[5] hydrogels,[6] meshes/nanofibers, and microspheres,[7] with each structure having unique physical, chemical, and biological properties.

Sponges and hydrogels are the two most broadly used forms of biomaterials, constituting ~35% and 45% of biomaterials used in tissue engineering (based on search of biomaterials used in cartilage regeneration with keywords "sponge," "hydrogel," "microsphere," or "nanofibers" in journal of "biomaterials" and "tissue engineering" from 2000 to 2011). Many biomaterials, including natural or synthetic polymers or their combinations, are fabricated into sponges

[1]Department of Biomedical Engineering, College of Engineering, Peking University, Beijing, People's Republic of China.
[2]Tissue Engineering Program, Life Sciences Institute, National University of Singapore, Singapore, Republic of Singapore.
[3]Center for Biomedical Materials and Tissue Engineering, Academy for Advanced Interdisciplinary Studies, Peking University, Beijing, People's Republic of China.
[4]Wallace H. Coulter Department of Biomedical Engineering, Georgia Institute of Technology, Atlanta, Georgia.
[5]Division of Bioengineering, School of Chemical and Biomedical Engineering, Nanyang Technological University, Singapore, Republic of Singapore.

or hydrogels and have shown impressive and unique properties in cartilage regeneration. For example, poly(lactic-co-glycolic acid) sponges modified with hyaluronic acid promoted chondrocyte functions with regard to adhesion, proliferation, glycosaminoglycan (GAG), and collagen II accumulation.[8] The hybrid sponges of collagen and chitosan, providing an extracellular matrix (ECM)-like environment to cartilage, enhanced cell attachment and subsequent cartilage formation.[9,10] Hydrogels, including polyethylene glycol (PEG), gelatin, alginate, and chitosan, also facilitated cartilage formation *in vitro*. PEG hydrogels with either hydrolysable units[11] or bioactive peptides[12] improved proliferation and ECM production for cartilage tissue growth. Chitosan-glycerophosphate (GP)/blood hydrogel implants were used to recruit cells[13] and were also applied as an injectable cell delivery vehicle.[14] Filling hydrogels into sponges has also been reported as a very efficient scaffold for the maintenance of chondrocyte phenotype and sustained mechanical support for the cartilage regeneration.[15] However, the mechanisms involved remain largely unexplored, as there is a lack of direct comparison of hydrogels and sponges for cartilage regeneration.

Sponges are porous structures whose properties are determined by interconnectivity, pore size, and porosity, which impact cell penetration and migration, matrix deposition and distribution, and nutrient and waste exchange.[16] A hydrogel is a network of polymer chains that are hydrophilic, swollen polymer matrices with a cross-linked structure and which retains a large amount of water.[17] Sponges are defined by morphology, while hydrogels are defined by hydrophobicity. In this current study, we adopt a well-accepted consensus that hydrogels are made of hydrophilic materials with water contact angles less than 60°, while sponges are porous structures made of materials with a water contact angle of 80° or above.[18–20]

As a polysaccharide similar to GAGs, chitosan has been widely used in cartilage regeneration. It can be fabricated into sponges by being lyophilizied and cross-linked with NaOH/ethonal[21] or into hydrogels by adding β-sodium glycerophosphate.[14,22] In this study, we investigated the effects of the physical properties of the chitosan sponges and hydrogels on the phenotypes of chondrocytes and the influence on cartilage generation, while maintaining similar material chemical properties. Functionalities of the cells in sponges and hydrogels were evaluated with regard to distribution, aggregation and morphology of the cells, as well as gene expression and ECM production.

Materials and Methods

Fabrication of sponges and hydrogels of chitosan

Three percent of chitosan [poly(β-(1-4-2-amino-2-deoxy-D-glucopyranase)] (Degree of deacetylation 80%–95%; viscosity 50–800 mPa.s; pH3.5,69047460, Guoyao Chemical Reagents Limited) solution was made by dissolving chitosan powder in 2M acetic acid. The solution was frozen at −80°C and lyophilized, before being rehydrated and hardened with NaOH/ethanol mixture and lyophilized again. The sponges were sterilized with 75% ethanol and rinsed with PBS until use in cell culture. The chitosan hydrogels were made by mixing filter-sterilized β-sodium GP (Sigma, molecular weight 216.04) with 3% chitosan and 10% GP. The acquired chitosan-GP solution was incubated at 37°C for 15–30 min to form a hydrogel.

Characterization of the sponges and hydrogels of chitosan

The freeze-dried scaffolds were immersed in PBS at 37°C for 2 h until equilibrium, before swelling ratio was measured. The swelling ratio was calculated as ER(ER = (Ws − Wd)/Wd, where Ws and Wd represent the weight of the swollen and dried scaffolds, respectively).[23] Porosity was estimated by immersing the scaffolds in absolute alcohol for 2 h. Porosity was calculated as follows: Porosity = (Ws − Wd)/ρ/V, where ρ was the density of alcohol and V was the volume of the scaffolds; Ws and Wd represent the weight of the swelling and dried scaffolds, respectively.[22] The morphologies of the sponges and fresh fabricated hydrogels were observed by environmental scanning electron microscopy (AMRAY-1910FE).

Mechanical properties

The compression test was performed on an Instron 5843 mechanical test (Instron Corporation). After preloading thrice to 10% of the strain, the freshly fabricated hydrogels and sponges were loaded at a constant speed of 0.1 mm/min to 20% of the strain. The Young's modulus was calculated using $E = \sigma/\varepsilon$ and $\varepsilon = 1 - L/L_0$, where L, L_0 represent the thickness before and after compression, separately. σ and ε were the stress and strain of the scaffold, respectively. Experiments were carried out in triplicate.

Bromophenol blue and bovine serum albumin diffusion

Three percentage of bromophenol blue (B-0126, Sigma) solution was added dropwise to the surface of the sponges and freshly fabricated hydrogels, respectively. The diffusion of bromophenol blue was photographed at 0, 0.5, 1, and 2 h. Release of bovine serum albumin (BSA, A-7030, Sigma) from sponges and hydrogels was detected with Coomassie brilliant blue G250 (Amresco) at 37°C. To prepare the BSA-loaded scaffolds, the BSA was mixed with chitosan-GP solution to yield BSA-loaded hydrogels; the same amount of BSA was dissolved in water, absorbed by dry sponges, and lyophilized to produce BSA-loaded sponges. Briefly, 100 μL of the incubated solution were taken out for measurement at 15 min, 30 min, 1, 2, 3, 3.5, 4, and 5 h. One hundred microliter of PBS was added to the incubated solution after taking out 100 μL solution. The experiment was performed in triplicate.

Culture of primary chondrocytes

Chondrocytes were harvested from knee joints of pigs (Yorkshire, 10–12 months). Articular cartilage was excised and digested with 0.15% collagenase II (Sigma) for 12 h with intermittent rotation. The acquired chondrocytes were cultured on tissue culture polystyrene with Dulbecco's modified Eagle medium (DMEM), (12800017, Gibco) containing 10% fetal bovine serum, 100 IU/mL penicillin, and 100 μg/mL streptomycin at 37°C in 5% CO_2. Medium was changed at 3 days' interval until 80% confluence was reached.

Two hundred thousand chondrocytes of passage 2 were seeded onto the sponge (5 × 5 × 2 mm), while 1×10^6 cells were seeded into 250 μL of hydrogels to keep the same cell

density (4×10^6 cells/mL) in the two scaffold systems. The chitosan-GP solution mixed with cells was incubated at 37°C for 30 min to gel, before 1 mL of medium was added. Medium was changed at 2 h. All the results from hydrogels were divided by five to compare with sponges. One milliliter of medium was added to cell-seeded sponges after 2 h incubation. All the scaffolds were cultured in 24-well plates, and culture medium was changed at 3 days' interval.

Cytotoxicity, proliferation, viability, and morphology of the chondrocytes

The cytotoxicity of the sponges and hydrogels was evaluated with 3-(4,5-Dimethyl-2-thiazolyl)-2,5-diphenyl-2H-tetrazolium bromide (MTT, M 2128, Sigma). Briefly, five thousand of chondrocytes were seeded in 96-well plates; then, 100 uL of culture medium was added. After 6 h, the sterilized latex rubber, hydrogels (50) μL, and sponges ($5\times5\times2$ mm) were added to the plate. The latex rubber was used as a positive control. The medium was changed every day. Absorbance was detected with a plate reader at 570 nm at 1 and 3 days. Four replicates were done.

Proliferation of the chondrocytes in the sponges and hydrogels was also evaluated with MTT (M 2128, Sigma). Five thousand of chondrocytes were seeded onto the sponges ($5\times5\times2$ mm) or mixed with 50 μL of hydrogel before 100 μL of culture medium was added. Medium was changed every day. Absorbance was detected with a plate reader at 570 nm at 1, 4, and 7 days. Four replicates were done.

For live–dead assay, the cells in scaffolds and hydrogels were stained with 2 μg/mL Fluorescein Diacetate (F7378, Sigma) at 37°C for 15 min and 5 μg/mL of Propidium Iodide (PI, P4170, Sigma) for 5 min, before being evaluated with confocal laser scanning microscopy (CLSM, LSM510, Zeiss) at an excitation wavelength of 488 nm and an emission wavelength from 550 to 670 nm. For F-actin staining, the samples were fixed with 4% paraformaldehyde; permeated in 0.1% Triton X-100; and incubated with rhodamine-phalloidin (PHDR1, cytoskeleton). Nuclei were counter stained with 4′, 6-diamidino-2-phenylindole (Sigma).

Quantization of GAG

The cell-laden scaffolds were digested with 50 μg/mL protein K (H10091, Merck) over night before the GAG content of the digested solution was quantitated with the 1,9-dimethylmethylene blue (DMMB, 341088, Sigma) colorimetric method, and the absorbance was measured at 630 nm.[24] Three replicates were done.

Real-time PCR

The cells were lysed with Trizol (15596-026, Invitrogen) before the total RNA was extracted according to the trizol's instructions. RNA concentration was determined using the Nano-Drop (Nano-Drop Technologies). The cDNA was synthesized by using iScript™cDNA synthesis kit (Bio-Rad) following the manufacturer's instructions. Real-time PCR was carried out with the Power SYBR Green PCR Master Mix (Applied Biosystem) on an Applied Biosystems 7500 Real-Time PCR System (Applied Biosystem) at 95°C for 15 m, 40 cycles of 15 s denaturation at 94°C, followed by 30 s annealing at 55°C, and 30 s elongation at 72°C. The target genes were normalized by the reference gene glyceraldehydes-3-phosphate dehydrogenase. The primers used for amplification were listed in Table 1. Triplicates were carried out.

In vivo *studies*

The *in vivo* animal experiment was approved by the Institutional Animal Care and Usage committee of the Peking University. Male athymic mice (6–7 weeks, SPF, Vital River) were used for the *in vivo* study. Ketamine (2.5 mg/mL, 50 mg/kg) was given by an intramuscular injection before three mid-sagittal skin incisions (5 mm) on the back of the mice were made. The cell-scaffold constructs, which had undergone 7 days *in vitro* culture, were implanted into the subcutaneous cavities. The incisions were treated with penicillin powder and then sutured. The constructs were harvested after implantation for 2 and 4 weeks.

Histology and immunohistochemistry

The harvested samples were fixed in 4% paraformaldehyde buffer (pH7.4) before being dehydrated, embedded in paraffin, and sectioned at 5 μm. For alcian blue staining, the sectioned samples were stained with 0.5% of alcian blue (Sigma-Aldrich) in 0.1 M HCl for 30 min and counter stained with fast red (Sigma-Aldrich). For immunohistochemistry, the sections were incubated with hydrogen peroxide and pepsin for 20 min, respectively, before being incubated with monoclonal antibodies of collagen type II (Clone 6B3; Chemicon, Inc.), collagen type I (Sigma C2456), and collagen type X (Clone×53, Quartett). After the incubation of biotinylated goat anti-mouse (Lab Vision Corporation) for 30 min, the slides were stained with a sequential incubation of streptavidin peroxidase, while 3, 3′-Diaminobenzidine was used as a chromogenic agent. The slides were covered and examined with a microscope (DM6000M, Leica). Both GAG and collagen II content were measured and compared with regard to mean optical density. The secreted GAG and collagen II of chondrocytes were evaluated with IPP software.

Statistical analysis

Student's *t*-test was applied to analyze the difference between each group, and all data were expressed as mean ± standard deviation with the significance level set at $p<0.05$.

Results

Characterization of sponges and hydrogels

The interior morphology of the sponges was a highly porous structure with interconnecting pores with a porosity of 53.2% ± 2.74% (Fig. 1a),while the hydrogels were also a porous structure but the pore size was much smaller and less interconnected (Fig. 1b). Swelling ratios of the dry hydrogels were 5.8 ± 0.703 at 37°C. The Young's modulus of the sponges (195.3 kPa) was significantly higher than that of hydrogels (2.0 kPa) ($p<0.01$).

Diffusion of bromophenol blue and BSA

Bromophenol blue diffused more quickly in sponges than in hydrogels (Fig. 2A). The dye distributed evenly throughout the entire sponges after 1 h, while dye distribution in the hydrogels remained partial after 2 h, with the edge of the hydrogel devoid

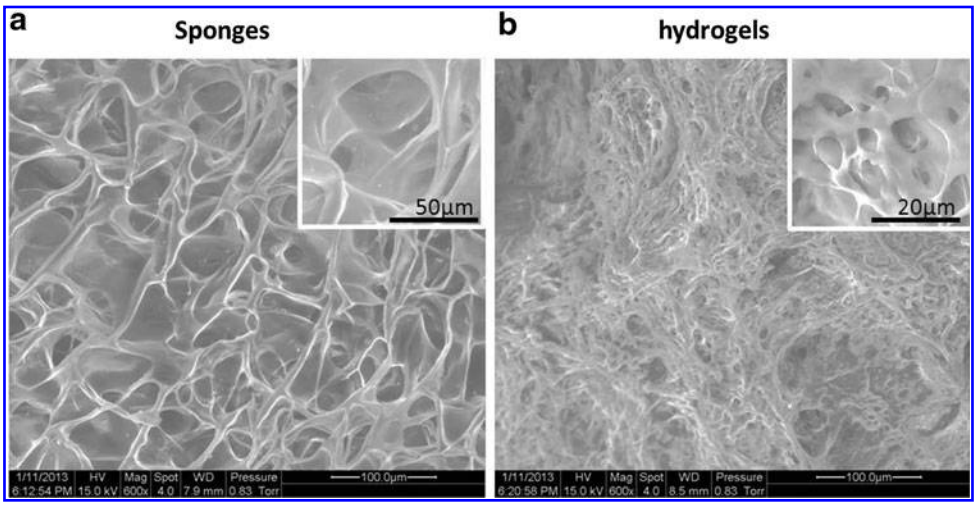

FIG. 1. Environmental scanning electron micrographs. **(a)** chitosan sponges, **(b)** chitosan hydrogels.

of dye. However, there was no significant difference between the release of BSA from the hydrogels and the sponges; it took 1 h for both of them to reach a peak concentration (Fig. 2B), and the release remained comparable with prolonged incubation.

Morphology and distribution of the chondrocytes

One day after seeding, the chondrocytes in sponges were elongated with aligned F-actin in the cytoplasm (Fig. 3a); whereas the chondrocytes in hydrogels had a round morphology with no obvious actin staining (Fig. 3b). The chondrocytes in the sponges remained elongated with increased aligned F-actins at day 7 (Fig. 3c), while the actin fibers of the chondrocytes were nearly not visible in the hydrogels at day 7 (Fig. 3d). More clusters of the chondrocytes (usually <10) were found in sponges at day 7 compared with those at day 1. Comparatively, the chondrocytes in the hydrogels scattered homogeneously at both day 1 and 7.

Cytotoxicity, proliferation, and viability

Both hydrogels and sponges were biocompatible (Fig. 4). The chondrocytes in sponges had a higher proliferation (Fig. 5). The cells proliferated significantly faster with time in the sponges ($p<0.01$), with a 1.6-fold increase at day 4 and almost a 1.8-fold at day 7, compared with day 1. However, the number of the chondrocytes did not change much in the hydrogels. The chondrocytes aggregated to form small

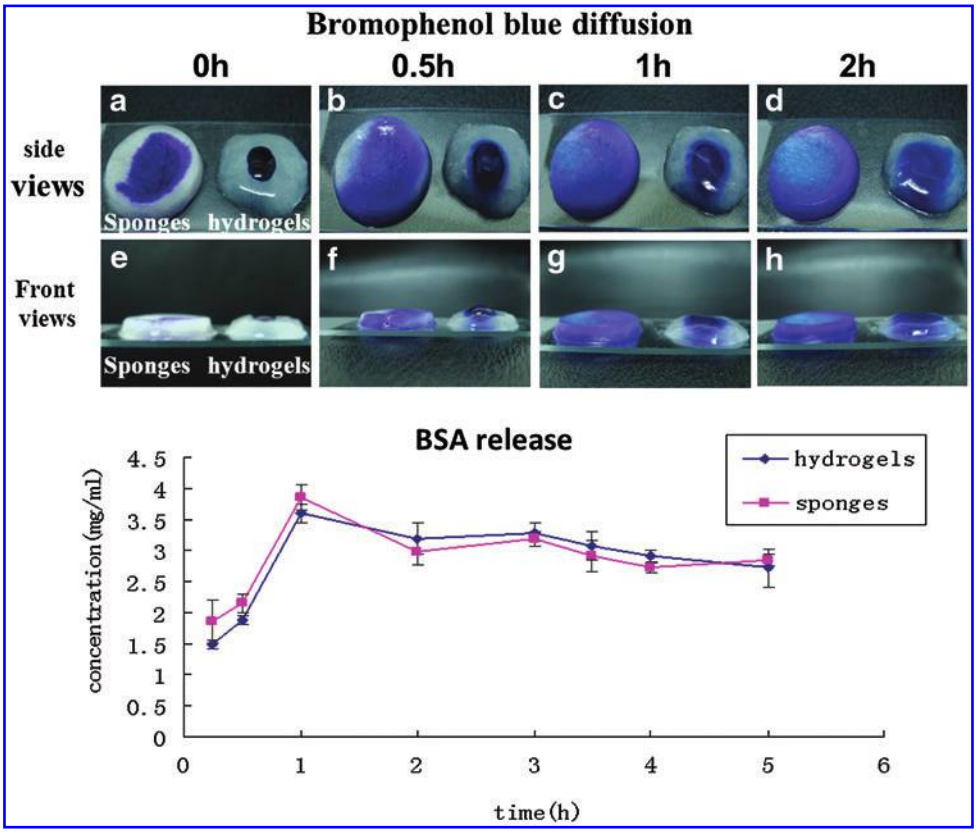

FIG. 2. The diffusion of bromophenol blue and release of bovine serum albumin (BSA). **(a)** The diffusion dynamics in the scaffolds in sponges (left) and hydrogels (right) Top views **(a, b, c, d)** and side views **(e, f, g, h)**. **(b)** Quantitative BSA release from the sponges and hydrogels ($n=3$). Color images available online at www.liebertpub.com/tea

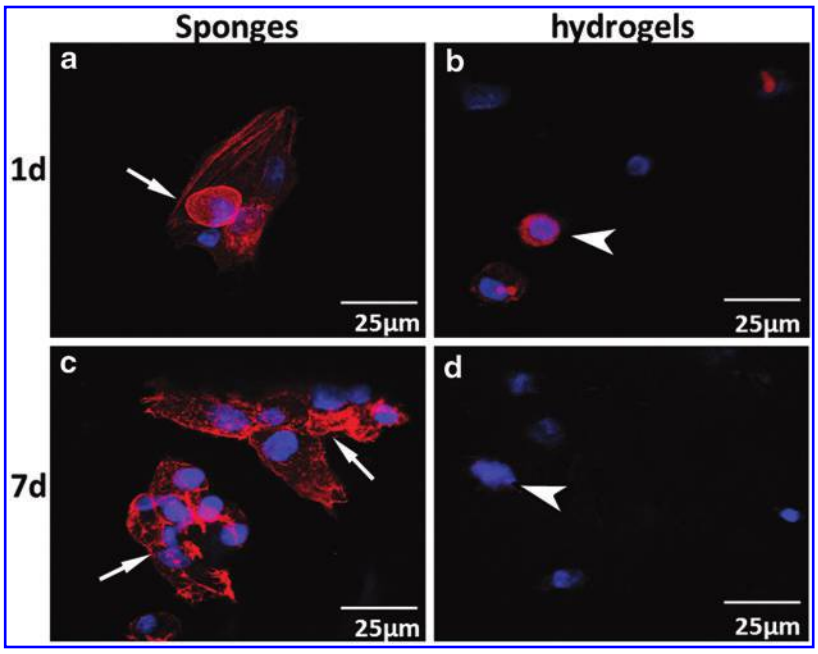

FIG. 3. Actin staining of the chondrocytes in the sponges **(a, c)** and hydrogels **(b, d)**. Actin was stained red, while the cell nucleus was blue. Arrow: stretched cell cytoskeletal and cell aggregation; Arrowhead: a round morphology and even distribution. Color images available online at www.liebertpub.com/tea

clusters in sponges, but distributed homogeneously in hydrogels at day 1 (Fig. 6a, b). Though the cell density in the two scaffolds (sponges and hydrogels) was kept identical at the time of seeding (Fig. 6a, b), the cell number increased dramatically and more cell clusters were observed at day 21 in the sponges (Fig. 6a, c); while the number of viable cells in the hydrogels remained nearly unchanged when compared with day 1 (Fig. 6b, d).

In vitro *histological and immunohistochemical studies*

The staining of both GAG and collagen type II was strong along the walls of the pores of the sponges, while it was homogeneous in hydrogels (Fig. 7). Except for the difference in distribution, there was no difference with regard to the staining density of GAG and collagen type II between sponges and hydrogels on both day 14 and day 28 (Supplementary Fig. S4; Supplementary Data are available online at www.liebertpub.com/tea). An analysis of GAG content by DMMB assays showed an increase in GAG in both hydrogels and sponges with time, but there was no significant difference between GAG content secreted by chondrocytes seeded on sponges and hydrogels on both day 14 and day 28 (Fig. 8).

Immunohistochemical staining for collagen I was strong and uneven in sponges, whereas it was homogenous and weak in hydrogels after 28 days. As for collagen X staining, there was nearly no staining in both sponges and hydrogels (Fig. 9).

Quantitative real-time PCR

Expression of collagen type I increased significantly with time in sponges ($p=0.03$), while it decreased with time in hydrogels. Though expression of collagen type I in the sponges and hydrogels was comparable at day 14, collagen type I expression was significantly lower in the hydrogels than in the sponges after 28 days ($p=0.01$) (Fig. 10A).

Expression of collagen type II in both the sponges and the hydrogels increased with time; however, time-dependent increase was only significant for hydrogel samples ($p=0.01$) (Fig. 10B).Expression of collagen type II in sponges was higher than in hydrogels on day 14 and day 28, but due to high standard deviation among samples in sponges, the differences were not significant.

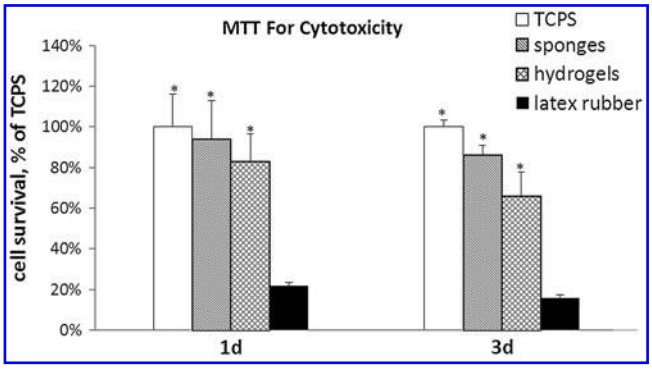

FIG. 4. 3-(4,5-Dimethyl-2-thiazolyl)-2,5-diphenyl-2H-tetrazolium bromide (MTT) test for cytotoxicity. Data were normalized as the percentage of Tissue Culture Plate Surface (TCPS). *$p<0.05$ compared with the latex rubber group ($n=4$).

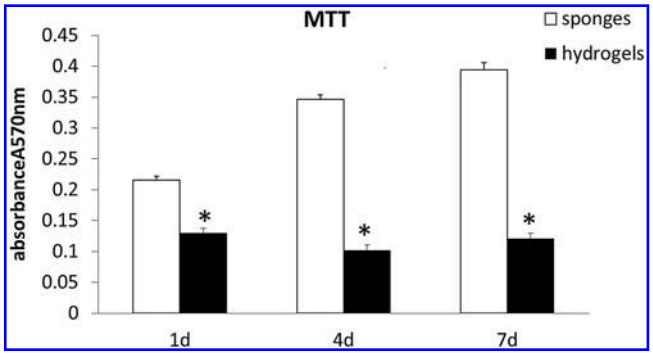

FIG. 5. Proliferation of the chondrocytes in the sponges and hydrogels. *$p<0.05$ compared with sponges ($n=4$).

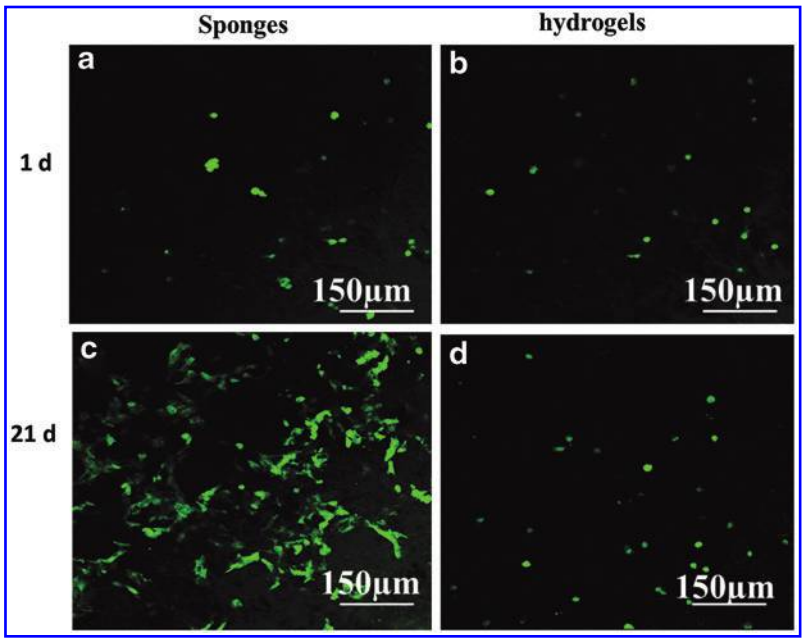

FIG. 6. The viability of the chondrocytes by fluorescein diacetate (FDA)-PI staining. Confocal microscopy photographs of FDA-PI staining image showed chondrocytes on the surface of sponges at **(a)** 1 day and **(c)** 21 days and in hydrogels at 1 day **(b)** and 21 days **(d)** after cell seeding. The live cells were dyed by FDA (green), and the dead cells were stained by PI (red). Color images available online at www.liebertpub.com/tea

Expression of aggrecan remained stable in sponges, while it increased significantly with time in hydrogels ($p=0.006$). Though expression of aggrecan showed no significant difference at 14 days, it was significantly higher in the hydrogels than in the sponges at 28 days ($p=0.01$) (Fig. 10C).

In vivo *histology*

Excretion of both GAG and collagen II increased with time, as indicated by Alcian Blue and collagen II staining. Staining of both GAG and collagen II was inhomogeneous in sponges with localized intense staining, while the staining was homogeneous in hydrogels. No significant difference of either GAG or collagen II was found between the sponges and hydrogels (Fig. 11).

There was neither collagen I nor collagen X staining after 2 weeks, while only weak homogenous staining was found after 4 weeks in hydrogels. On the other hand, the staining for collagen I and collagen X was positive after 2 weeks in sponges, while the staining for collagen I and collagen X became strong in the sponges at week 4. This staining was much stronger than that in the hydrogels (Fig. 12).

Discussion

The scaffolds with various internal structures provide different micro-environments for the cells. The cells can recognize their microenvironments, and they selectively activate or down-regulate genes and modify their phenotypes accordingly.[25–27] The scaffold microstructure can direct

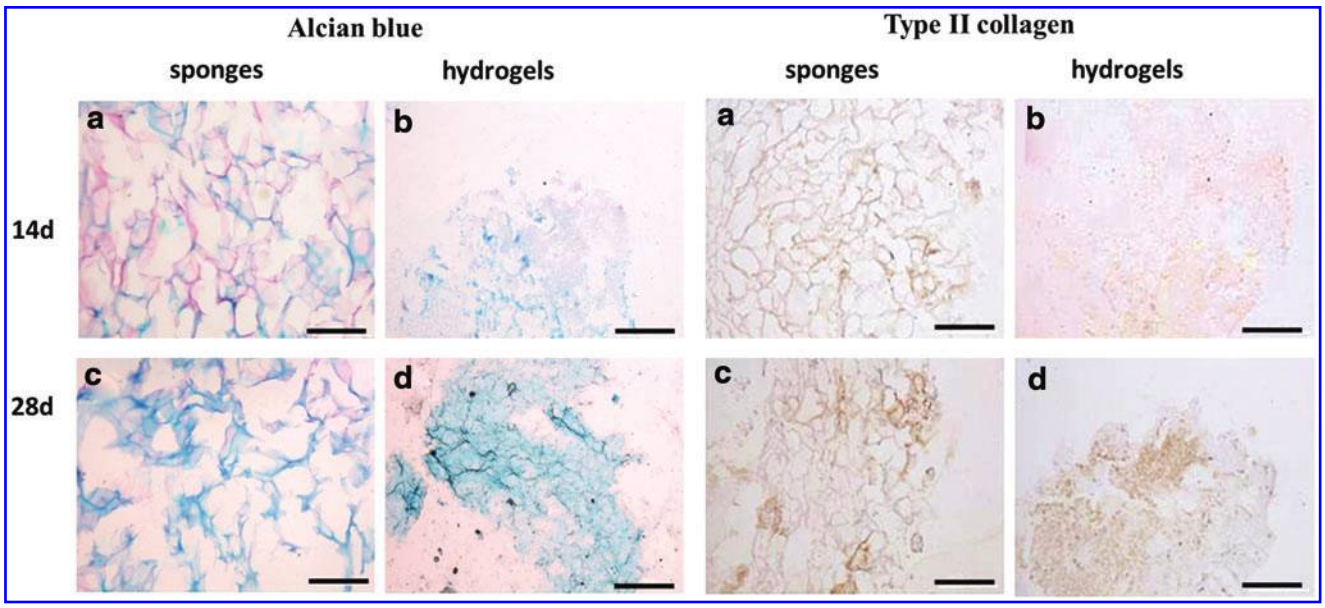

FIG. 7. Alcian blue staining and immunohistochemical staining for collagen II *in vitro*. (left) Alcian blue staining of sponges **(a, c)** and hydrogels **(b, d)**. (right) Collagen II immunohistochemical staining for sponges **(a, c)** and hydrogels **(b, d)**. Scale bars: 100 μm. Color images available online at www.liebertpub.com/tea

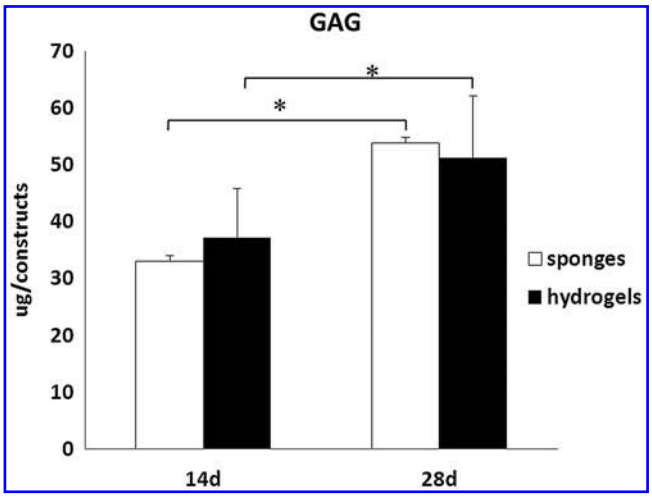

FIG. 8. GAG content on day 14 and day 28 after seeding in hydrogels and sponges (*$p < 0.05$, $n = 3$). GAG, glycosaminoglycan.

cell morphology, cytoskeletal organization, proliferation, and matrix production through chemical, biological, physical, and mechanical factors.

In this study, chitosan fabricated in the form of sponges and hydrogels is comprehensively investigated and compared as the scaffolds for supporting cartilage formation with chondrocytes. Both forms of the scaffold in this study were fabricated with the same batch of chitosan, thus eliminating chemical composition as a possible influence for the different results. We also minimized the variation of cell density by seeding the same cell number per volume for both scaffolds. The effect of GP can also be excluded, as the chitosan-GP sponge did not alter the morphology and distribution of chondrocytes (Supplementary Fig. S2), and the gene expression of collagen II and sox 9 was lower in hydrogel, but no significant difference was found between these two groups (Supplementary Fig. S3). Cell-loading method contributed much to the aggregations in the sponges as cell suspension was dropped onto the surface of the sponge and was allowed to seep through by gravitational force, and cell distribution was constrained by the interconnectivity of the sponges. On the other hand, the cells distributed as single cells homogenously throughout the hydrogels as cells were mixed thoroughly with the material before hydrogel formation.

At the cellular levels, the chondrocytes showed a spindle morphology with stressed F-actin fibers in the sponges, differing from that in the hydrogels. The cells that attached onto the pores of the sponges were similar with what happened in a 2D microenvironment (Fig. 13). The chondrocytes that were embedded in the chitosan hydrogels kept round morphologies, as the cells could sense the materials all around them. Integrin-mediated cell attachment might play a key role in this process. Cell functions are strongly associated with cell morphology, which is affected by the structural format of the biomaterials. It was shown that chondrocytes on a nano-fibrous scaffold formed a globular-shaped morphology and produced more cartilage-specific ECM such as GAG and collagen type II, when compared with a well-spread, fibroblast-like shape of chondrocytes on a micro-fibrous scaffold.[28]

In our study, the altered phenotypes are associated with varied morphologies of the cells and varied gene expression due to the different internal structures of the scaffolds. The strong expression of collagen type I was detected in chondrocytes residing in the sponges, showing signs of de-differentiation. Enhanced cell proliferation in the sponges further hinted at de-differentiation of the chondrocytes in the sponges, as fully differentiated chondrocytes were known to undergo little proliferation,[29] a phenomenon that is also observed in our chondrocytes in the hydrogels. Scaffold structure may impact nutrient diffusion, which might affect cell proliferation, as sponges provided larger interconnected pores while hydrogels had less porous structure with a smaller pore size.

More chondrogenesis was seen in the outer regions of the sponges, while the matrix accumulated homogeneously throughout the hydrogels. The cells in both the sponges and hydrogels produced a similar amount of GAG, despite

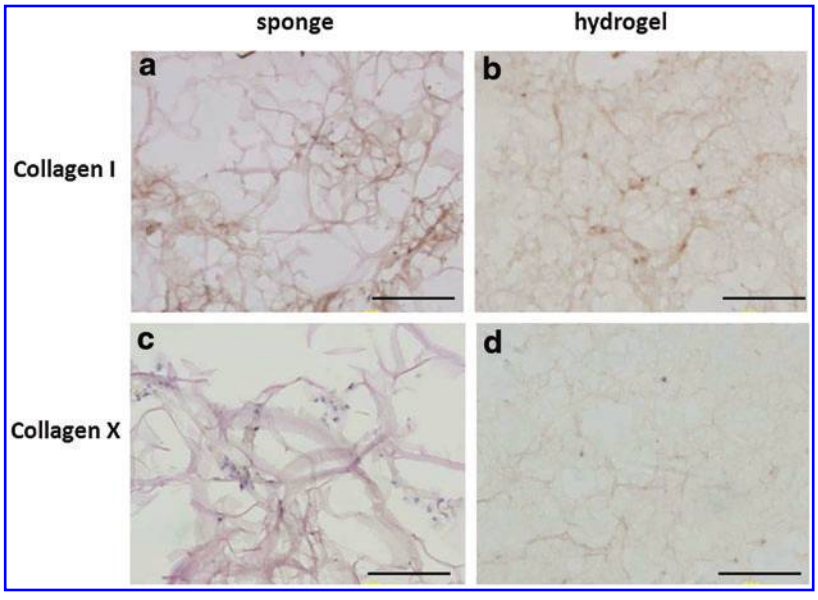

FIG. 9. Immunohistochemical staining for collagen type I and collagen type X for *in vitro* scaffold constructs at day 28. **(a)** collagen type I staining of the sponges. **(b)** collagen type I staining of the hydrogels. **(c)** collagen type X staining of the sponges. **(d)** collagen type X staining of the hydrogels. Scale bars: 100 μm. Color images available online at www.liebertpub.com/tea

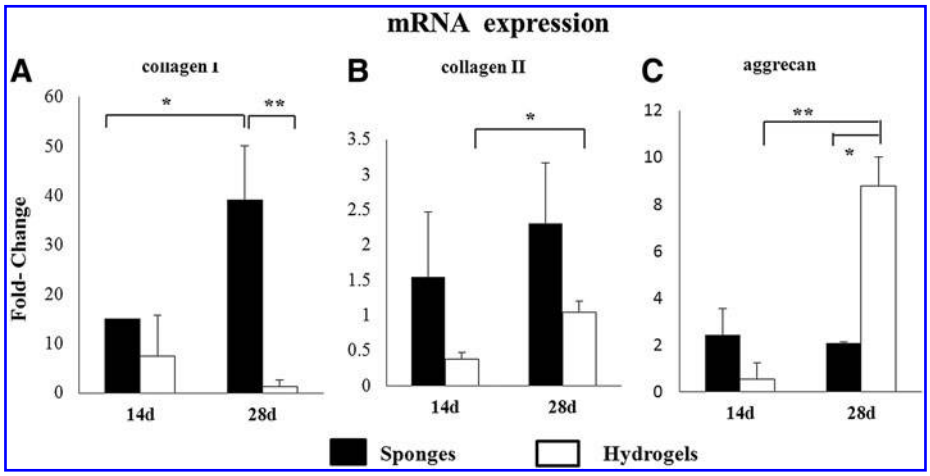

FIG. 10. The mRNA expression of collagen type I **(A)**, collagen type II **(B)**, and aggrecan **(C)** *in vitro* (*$p < 0.05$, and **$p < 0.01$, $n = 3$).

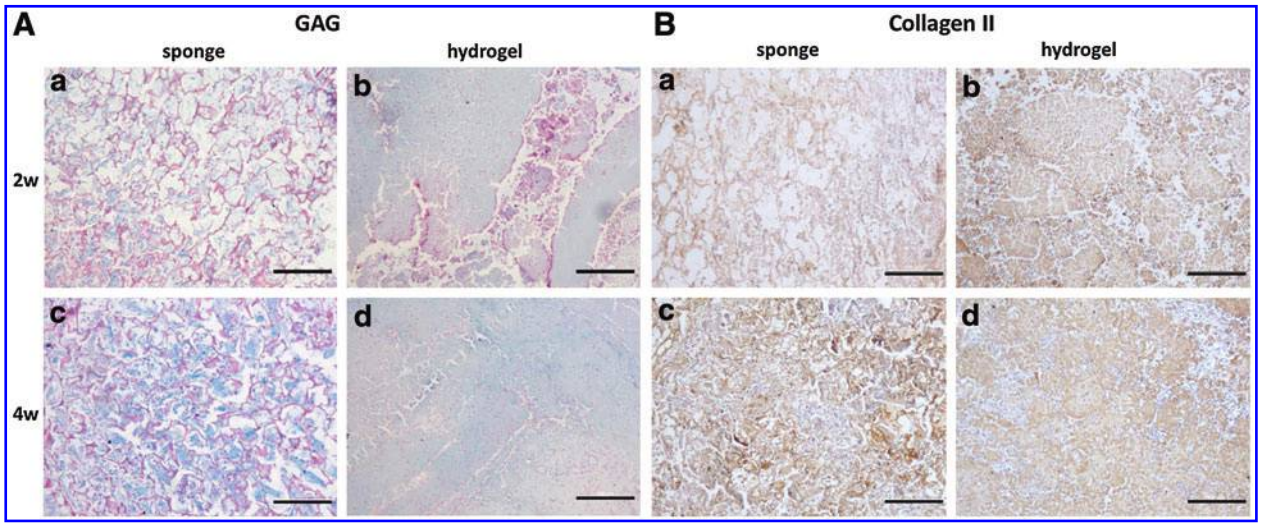

FIG. 11. Alcian blue staining and immunohistochemical staining for collagen II *in vivo*. The constructs were cultured for 1 week *in vitro* before being transplanted into mice subcutaneous cavities for another 2 weeks and 4 weeks. **(A)** Alcian blue staining of sponges **(a, c)** and hydrogels **(b, d)**. **(B)** Collagen II staining for sponges **(a, c)** and hydrogels **(b, d)**. Scale bars: 100 μm. Color images available online at www.liebertpub.com/tea

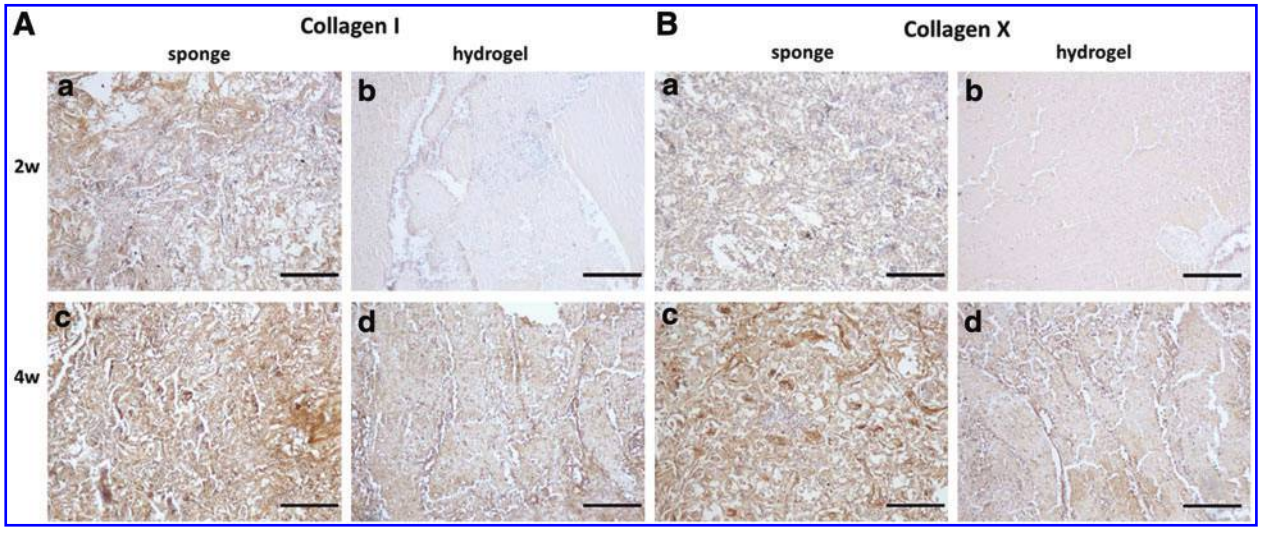

FIG. 12. Immunohistochemical staining for collagen I and collagen X for *in vivo* scaffold constructs. The constructs were cultured for 1 week *in vitro* before being transplanted into mice subcutaneous cavities for another 2 weeks and 4 weeks.**(A)** Collagen I staining for sponges **(a, c)** and hydrogels **(b, d)**. **(B)** Collagen X staining for sponges **(a, c)** and hydrogels **(b, d)**. Scale bars: 100 μm. Color images available online at www.liebertpub.com/tea

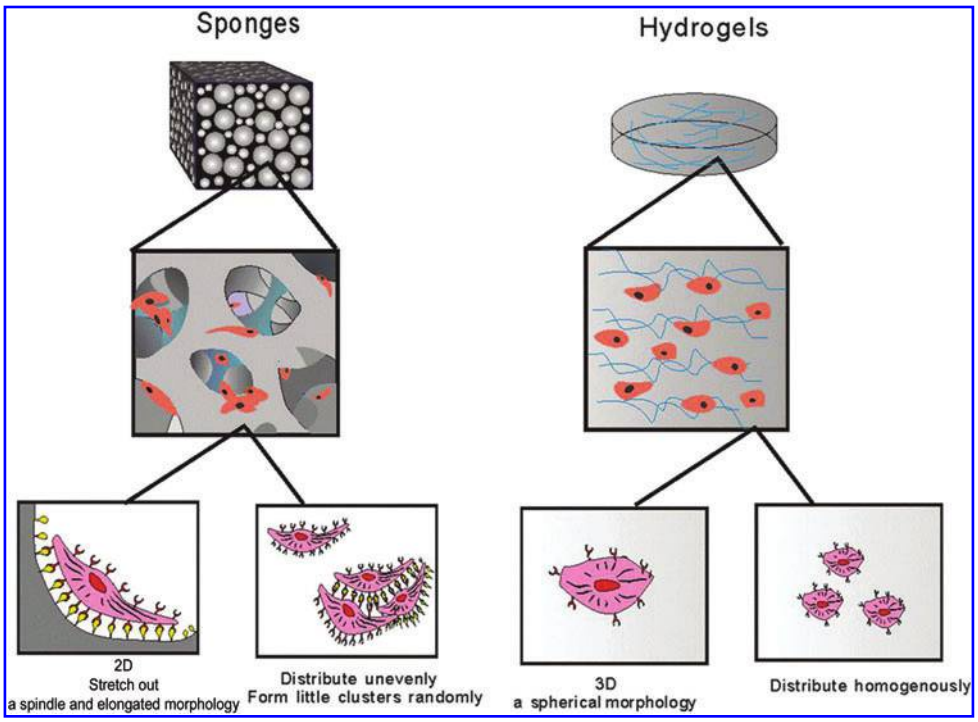

FIG. 13. The schematic illustration of different behaviors of chondrocytes in sponges and hydrogels. Chondrocytes tended to stretch out and form little clusters in sponges (left), while they maintained a round morphology and were distributed evenly within hydrogels (right). Color images available online at www.liebertpub.com/tea

the difference in cellular morphology and proliferation status. The cells were fully differentiated and nearly did not proliferate in the hydrogels, while the cells proliferated quickly and partially dedifferentiated in the sponges. The aggregation of the chondrocytes in the porous sponges could enhance chondrogenesis through cell–cell contact and contribute to ECM accumulation.[30] Cell aggregation may also partially offset the dedifferentiation caused by chondrocyte attachment and subsequent morphological changes through enhanced cell–cell interactions. Notably, not all cells in the sponge were in clusters, while some of them attached onto the materials. This might explain the high standard deviation in the mRNA analysis in the sponge samples.

Collagen type X, a marker for chondrocyte hypertrophy, was low in both sponges and hydrogels, indicating no hypertrophy in both scaffolds *in vitro*. Staining of both collagen type I and collagen type X was enhanced in the subcutaneous implanted sponges, which indicated the inferior phenotype of the chondrocytes in the sponge than that in the hydrogel (Fig. 12). The subcutaneous implantation could not mimic the real cartilage environment and might give the wrong signals for cartilage regeneration. Cell–sponge constructs, implanted into the subcutaneous cavities, were easily affected by the surroundings because of the large pores and interconnected structures and resulted in an inferior phenotype of chondrocytes. However, the chondrocytes embedded in the hydrogels tended to maintain phenotypes due to the relatively inert property caused by the smaller pores and less interconnected structure. Thus, the cell constructs might be implanted to repair cartilage defects instead of the subcutaneous cavities to further compare these two scaffolds.

A better understanding of the cellular behaviors in sponges and hydrogels can provide insights regarding the design of scaffolds for cartilage regeneration. The results indicated that hydrogels could be used to maintain chondrocyte phenotypes, while the expansion of chondrocytes can be achieved in sponges. In future, a hybrid scaffold that incorporates features which encourage chondrocyte proliferation with a differentiation-enhancing capacity will better serve cartilage regeneration.

Table 1. Primer Sequences for Chondrogenic Marker Genes

Target	*Primer sequence forward and reverse (5′→3′)*
GAPDH	ATGGTGAAGGTCGGAGTGAA; AATGAAGGGGTCATTGATGG
Aggrecan	CATCACCGAGGGTGAAGC; CCAGGGGCAAATGTAAAGG
Type I Collagen	CAGAACGGCCTCAGGTACCA; CAGATCACGTCATCGCACAAC
Type II Collagen	TGAGAGGTCTTCCTGGCAAA; GAAGTCCCTGGAAGCCAGAT
Type X Collagen	TGCTGCTGCTATTGTCCTTG; TGAAGAACTGTGCCTTGGTG

Conclusion

Chondrocytes showed heterogeneous morphologies, clustered or attached to the materials with a spindle-like morphology in the sponges, while they distributed evenly and displayed homogeneous, spherical morphologies in the hydrogels. A higher proliferation accompanying an elevated expression of collagen type I was found in sponges when compared with good phenotype associated up-regulated expression of aggrecan in the hydrogels. In general, the overall performance of the chondrocytes in the sponges and the hydrogels is comparable, as testified with equivalent ECM depositions. It is reasonable to optimize the biomaterials through harnessing merits from both the sponges and the hydrogels.

Acknowledgments

The authors would like to acknowledge support from the National Basic Research Program of China grant (973 Program) (2012CB619100), as well as the National Natural Science Foundation of China grant (81271722).

Disclosure Statement

The authors declare that they have no competing interests.

References

1. Grayson, W.L., *et al.* Engineering custom-designed osteochondral tissue grafts. Trends Biotechnol **26,** 181, 2008.
2. Ge, Z.G., *et al.* Osteoarthritis and therapy. Arthritis Rheum-Arthritis Care Res **55,** 493, 2006.
3. Alford, J.W. Cartilage restoration, part 1: basic science, historical perspective, patient evaluation, and treatment options. Am J Sports Med **33,** 295, 2005.
4. Alford, J.W. Cartilage restoration, part 2: techniques, outcomes, and future directions. Am J Sports Med **33,** 443, 2005.
5. Liumin, H., *et al.* Microstructure and properties of nanofibrous PCL-b-PLLA scaffolds for cartilage tissue engineering. Eur Cells Mater **18,** 63, 2009.
6. Ladet, S.G., *et al.* Multi-membrane chitosan hydrogels as chondrocytic cell bioreactors. Biomaterials **32,** 5354, 2011.
7. Choi, S.W., *et al.* Uniform beads with controllable pore sizes for biomedical applications. Small **6,** 1492, 2010.
8. Yoo, H.S., *et al.* Hyaluronic acid modified biodegradable scaffolds for cartilage tissue engineering. Biomaterials **26**, 1925, 2005.
9. Yan, L.-P., *et al.* Genipin-cross-linked collagen/chitosan biomimetic scaffolds for articular cartilage tissue engineering applications. J Biomed Mater Res Part A **95A,** 465, 2010.
10. Gong, Z., *et al.* Use of synovium-derived stromal cells and chitosan/collagen type I scaffolds for cartilage tissue engineering. Biomed Mater **5,** 055005, 2010.
11. Rice, M.A., and Anseth, K.S. Encapsulating chondrocytes in copolymer gels: bimodal degradation kinetics influence cell phenotype and extracellular matrix development. J Biomed Mater Res **70A,** 560, 2004.
12. Lee, H.J., *et al.* Collagen mimetic peptide-conjugated photopolymerizable PEG hydrogel. Biomaterials **27,** 5268, 2006.
13. Chevrier, A., *et al.* Chitosan-glycerol phosphate/blood implants increase cell recruitment, transient vascularization and subchondral bone remodeling in drilled cartilage defects. Osteoarthritis Cartilage **15,** 316, 2007.
14. Hoemann, C.D., *et al.* Tissue engineering of cartilage using an injectable and adhesive chitosan-based cell-delivery vehicle. Osteoarthritis Cartilage **13,** 318, 2005.
15. Wang, W., *et al.* In vivo restoration of full-thickness cartilage defects by poly(lactide-co-glycolide) sponges filled with fibrin gel, bone marrow mesenchymal stem cells and DNA complexes. Biomaterials **31,** 5953, 2010.
16. Lee, S.-H., and Shin, H. Matrices and scaffolds for delivery of bioactive molecules in bone and cartilage tissue engineering. Adv Drug Deliv Rev **59,** 339, 2007.
17. Hoffman, A.S. Hydrogels for biomedical engineering. Adv Drug Deliv Rev **43,** 3, 2002.
18. Rathbone, S., *et al.* Biocompatibility of polyhydroxyalkanoate as a potential material for ligament and tendon scaffold material. J Biomed Mater Res Part A **93A,** 1391, 2010.
19. Ku, S.H., and Park, C.B. Human endothelial cell growth on mussel-inspired nanofiber scaffold for vascular tissue engineering. Biomaterials **31,** 9431, 2010.
20. McBane, J.E., *et al.* The effect of degradable polymer surfaces on co-cultures of monocytes and smooth muscle cells. Biomaterials **32,** 3584, 2011.
21. Yang, Z., *et al.* Improved mesenchymal stem cells attachment and in vitro cartilage tissue formation on chitosan-modified poly(l-lactide-co-epsilon-caprolactone) scaffold. Tissue Eng Part A **18,** 242, 2012.
22. Li, C., *et al.* A viscoelastic chitosan-modified three-dimensional porous poly(l-lactide-co-ε-caprolactone) scaffold for cartilage tissue engineering. J Biomater Sci Polym Ed **23,** 405, 2012.
23. Nair, S., *et al.* A biodegradable in situ injectable hydrogel based on chitosan and oxidized hyaluronic acid for tissue engineering applications. Carbohydr Polym **85,** 838, 2011.
24. Yin, J., Zheng, Y., and Zi-gang, G. Characterization of human primary chondrocytes of osteoarthritic cartilage at varying severity. Chinese Med J **124,** 4245, 2011.
25. Ragetly, G.R., *et al.* Effect of chitosan scaffold microstructure on mesenchymal stem cell chondrogenesis. Acta Biomater **6,** 1430, 2010.
26. Kumar, G., *et al.* The determination of stem cell fate by 3D scaffold structures through the control of cell shape. Biomaterials **32,** 9188, 2011.
27. Yang, Y., Wimpenny, I., and Ahearne, M. Portable nanofiber meshes dictate cell orientation throughout three-dimensional hydrogels. Nanomed Nanotechnol Biol Med **7,** 131, 2011.
28. Wan, J., Yi, J., and Rocky, S.T. Chondrocyte phenotype in engineered fibrous matrix. Tissue Eng **12**, 1775, 2006.
29. Elena Schun, M.S., and Jan Kramer, M.D. Effect of matrix elasticity on the maintenance of the chondrogenic phenotype. Tissue Eng **16,** 11, 2010.
30. Wolf, F., Candrian, C., and Wendt, D. Cartilage tissue engineering using pre-aggregated human articular chondrocytes. Eur Cells Mater **16,** 92, 2008.

Address correspondence to:
Zigang Ge, PhD
Department of Biomedical Engineering
College of Engineering
Peking University
Beijing
People's Republic of China, 100871

E-mail: gez@pku.edu.cn

Received: June 26, 2012
Accepted: April 16, 2013
Online Publication Date: June 6, 2013